IEEE Access
Multidisciplinary | Rapid Review | Open Access Journal

Received March 18, 2022, accepted April 11, 2022, date of publication April 18, 2022, date of current version April 26, 2022.

Digital Object Identifier 10.1109/ACCESS.2022.3168162

Photonic Spectrum Analyzer for Wireless Signals in the THz Range

BENEDIKT LEANDER KRAUSE, ANUAR DE JESUS FERNANDEZ OLVERA, AND SASCHA PREU, (Member, IEEE)

Department of Electrical Engineering and Information Technology, Institute of Microwave Engineering and Photonics, Terahertz Devices and Systems, Technical University of Darmstadt (TUDa), 64283 Darmstadt, Germany

Corresponding author: Benedikt Leander Krause (benedikt.krause@tu-darmstadt.de)

This work was supported by the European Research Council (ERC) through the Framework of ERC Starting Grant "Pho-T-Lyze" under Grant GA 713780.

ABSTRACT We present an ultra-broadband and inexpensive photonic spectrum analyzer (PSA) for wireless signals with a frequency coverage from the microwave range till deep into the terahertz range. The difference frequency of two continuous-wave laser diodes works as the local oscillator frequency and a photoconductive antenna downconverts a signal under test with the aid of the optical local oscillator. With this approach we achieve a frequency coverage from less than 25 GHz to more than 1.25 THz, mostly limited by the tuning range of the lasers. No component of our spectrum analyzer needs to be interchanged in order to achieve the full tuning range, which makes our spectrum analyzer a fraction of the cost of an electronic spectrum analyzer that requires several extension modules for covering a similar frequency range. The system offers a minimum resolution bandwidth of 1.2 MHz at a displayed average noise level (DANL) as low as −113.8 dBm/Hz at 100 GHz or as low as −88.2 dBm/Hz at 1050 GHz.

INDEX TERMS Photomixer, photonic local oscillator, spectrum analyzer, terahertz radiation.

I. INTRODUCTION

With the continuously rapid increase in mobile traffic volume, the data rate limits of 5G wireless transmission will soon be reached. To achieve higher data rates, 6G wireless communication will utilize the terahertz (THz) band (0.1 THz - 10 THz) with frequencies beyond 95 GHz and possibly even from 275 GHz to 3 THz [1]. The development of 6G-infrastructure, as well as components for many other Terahertz applications requires investigation of their spectral properties for confirming the simulated and targeted specifications. A common tool to perform this analyis is a spectrum analyzer (SA) that measures the spectral components emitted from a source or transmitted through a component. It can therefore analyze the signal purity, the presence of undesired (remaining fundamental signal components in multiplier chains or the IP3 point of amplifiers, e.g.) or desired mixing products (frequency multiplication, e.g.). For the frequency range beyond 100 GHz to frequencies above 1 THz five different SA achitectures have been demonstrated to date. Two are based on recording time domain traces followed by transformation to the frequency domain (e.g. Fourier transformation) and three on downconverting the signal with different local oscillators in the frequency domain.

An interferometer-based (e.g. Michelson or Martin-Puplett type) SA is reported in [2], [3]. The time trace of the self-homodyne interferogram generated by adding a delay in one of the two interferometer arms is Fourier transformed in order to obtain the spectral characteristics. The maximum travel of the delay stage, its accuracy and speed limit the obtainable frequency range, the resolution and the measurement time of this SA. A frequency range from 100 GHz up to 1.5 THz, a minimum resolution of 750 MHz and a dynamic range of 45 dB have been demonstrated [2], [3]. Despite being a fast and inexpensive architecture of an SA, the low resolution limits the SA to the detection of wideband or low coherence signals only.

The second SA is based on a Josephson junction and a Hilbert transformation with a frequency range from 30 GHz to 1 THz [4]. The electrical response of a Josephson junction irradiated by an incoming signal is proportional to the Hilbert transformation of the incoming signal. Therefore, the spectrum of a signal under test (SUT) can be determined with a reverse Hilbert transformation. While the Josephson

The associate editor coordinating the review of this manuscript and approving it for publication was Qingli Li.

junction can be tuned electrically, which allows for very fast measurement times, the junction needs to be in the superconductive state. State-of-the-art high TC superconductors in Josephson junctions still require temperatures below 80 K, requiring at least a closed loop stirling refrigerator or similar. This may also limit the maximum power of the signal to be analyzed. Systems that tolerate several mW power levels, as required for 6G systems, may need more powerful cryogenic systems based on liquid Nitrogen or even helium that may not be suitable for most electronics laboratories.

The most powerful and most frequently used commercial systems to date are electronic SAs (ESAs) with base units that have yet reached frequencies of up to 90 GHz [5]. For extension up to 1.5 THz frequency extenders based on multipliers are designed for rectangular hollow metallic waveguide standards [6]. Each extender module is limited to a certain frequency range determined by the cut-off of the hollow core waveguide and the emergence of higher order modes that do not comply with the multiplier architecture. In order to cover the full range from 90 GHz to 1.5 THz at least 6 extender modules are needed. The resolution bandwidth, the conversion losses, as well as the phase noise increase mostly superlinear with each multiplication step of the local oscillator generated by the base unit. Still, the phase noise and spectral resolution are outstanding, in the range of 1-10 Hz at the lower end of the THz spectrum [5], [6]. The minimum detectable power (equalling to the displayed average noise level (DANL) subtracted by the conversion loss) yet commercially achievable in the range of 1.1-1.5 THz is just below −110 dBm [5], [6]. This SA is very accurate but at the same time a high-cost option, which limits the accessibility of these systems, yet impeding large scale usage for component development.

Another SA architecture is based on down-convertion of the spectrum with the aid of a mode-locked laser (MLL) and a photoconductive antenna [7]. The photoconductor absorbs an optical beat signal resulting from heterodyning any two modes of the MLL that act as local oscillator, $\nu_{ij} = |\nu_i - \nu_j|$. At the same time, it receives the THz SUT at f_{THz} with the aid of an antenna where the THz field is converted to a bias that biases the photoconductor. The resulting RF beat signals at frequencies $f_{rf} = |\nu_{ij} - f_{THz}|$ are amplified and displayed using an ESA. Since the MLL has many frequencies, there are at least the same amount of mixing products. In order to detect a SUT uniquely, only the closest mixing product to DC is used. In order to determine which of the modes generated the signal closest to DC, the repetition rate f_{rep} of the MLL is varied slightly by a known amount. As modes with a mode number difference of N shift relatively in frequency by Nf_{rep}, monitoring the IF frequency change within the ESA allows to determine the respective line and hence the absolute frequency of the incoming signal [7], [8]. The frequency range of the SA is determined by the noise floor of the photoconductive antenna (PCA) and its frequency roll-off but also by the power of each modes of the MLL. This SA has been used up to 1.5 THz at least. The main limiting factor for this system is the difficulty of detecting arbitrary or broadband signals.

The above described SAs are either Fourier- or Hilbert-transformation based, which limits their resolution, or they are extensions to an ESA, which makes them expensive options. In a previous publication, we have demonstrated a true optoelectronic SA [9] without the requirement of an electronic SA, and a variant thereof [10] where a continuous-wave (CW) electro-optic (EO) comb was employed as local oscillator in conjunction with a 1550 nm-compatible photoconductor [11] as mixer. The comparatively inexpensive CW comb enabled a Hz-level spectral resolution as demonstrated in [9] in the microwave range (50 - 90 GHz) and [10] up to 340 GHz, yet with limitations on frequency coverage.

In this paper, we show a simple way to extend the frequency coverage beyond 1 THz by substituting the EO comb system by two tunable lasers, a setup commonly used in CW homodyne photomixing spectrometers. It is capable of analyzing any arbitrary signal within the frequency range of <25 GHz to potentially several THz. We demonstrate its functionality by analyzing signals from different sources between 100 GHz and 1 THz, being able to resolve signals with less than −60 dBm power. The SA is fully compatible with existing CW photomixing spectrometers, just requiring a few modifications on the detection chain.

II. PHOTONIC SPECTRUM ANALYZER ARCHITECTURE

Fig. 1 shows the general setup of the proposed photonic spectrum analyzer (PSA) [13]. It consists of four main components:

1) two telecom CW distributed feedback laser (DFB) laser diodes with temperature and current controller (TOPTICA Terascan DLC)
2) ErAs:InGaAs photoconductive mixer with integrated logarithmic-periodic antenna (PCA)
3) trans-impedance amplifier (TIA)
4) acquisition card (ACQC)

Optically isolated and polarization-maintaining fiber-coupled, free running C-band CW lasers emit laser signals with typical linewidths and stabilities of the order of 1 MHz at angular frequencies ω_1 and ω_2. Their difference frequency of $\omega_{\mathrm{L,THz}} = |\omega_1 - \omega_2|$ is chosen to lie in the lower THz range and serves as LO frequency. The wavelength of both lasers and therefore the LO frequency can be conveniently tuned by changing and controlling the temperature of the lasers. A 3-dB polarization maintaining fiber coupler heterodynes the two laser signals resulting in an envelope modulation at the beat signal $\omega_{\mathrm{L,THz}}$. The lasers are focused onto a PCA, which absorbs the signal and generates electron-hole pairs with a concentration $n(t)$ that follows the optical envelope, [14], [15]

$$n(t) \sim P_{\mathrm{L}}(t) = P_{\mathrm{L},0}(1 + \cos(\omega_{\mathrm{L,THz}} t + \varphi_{\mathrm{L,THz}})), \quad (1)$$

with $\varphi_{\mathrm{L,THz}}$ being the starting phase of the lasers. An on-chip planar antenna converts the received free-space electric field of the SUT, $E_{\mathrm{s,THz}}(t)$, into a bias voltage $U_{\mathrm{s,THz}}(t)$,

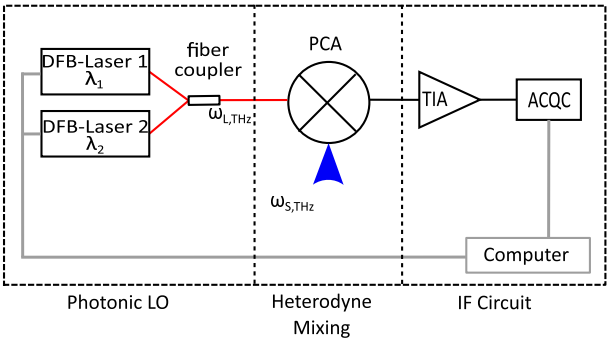

FIGURE 1. Schematic of the implemented photonic spectrum analyzer.

which modulates the carrier velocity $v(t)$. In case of a single frequency THz wave, the carrier velocity becomes

$$v(t) \sim U_{\mathrm{s,THz}}(t) \sim E_{\mathrm{s,THz}}(t) = E_{\mathrm{s,THz}} \cos(\omega_{\mathrm{s,THz}} t + \varphi_{\mathrm{s,THz}}), \tag{2}$$

with $\varphi_{\mathrm{s,THz}}$ being the starting phase of the SUT. Arbitrary, broadband signals will be discussed later on the basis of a spectral decomposition. We remark that (2) assumes Ohm's law which may not be fulfilled on the time scale of a THz period but still provides a decent approximation.

The photoconductor generates a current corresponding to the convolution of the bias and the conductivity. For the single frequency case, the convolution turns into a product, yielding sum and difference frequency mixing components,

$$\begin{aligned} I(t) &\sim n(t)v(t) \sim \cos(\omega_{\mathrm{s,THz}} t + \varphi_{\mathrm{s,THz}}) \\ &\quad + \eta \cos(\omega_{\mathrm{L,THz}} + \varphi_{\mathrm{L,THz}}) \cos(\omega_{\mathrm{s,THz}} t + \varphi_{\mathrm{s,THz}}) \\ &= \cos(\omega_{\mathrm{s,THz}} t + \varphi_{\mathrm{s,THz}}) \\ &\quad + \frac{1}{2}\eta(\cos((\omega_{\mathrm{L,THz}} + \omega_{\mathrm{s,THz}})t + \varphi_{\mathrm{L,THz}} + \varphi_{\mathrm{s,THz}}) \\ &\quad + \cos((\omega_{\mathrm{L,THz}} - \omega_{\mathrm{s,THz}})t + \varphi_{\mathrm{L,THz}} - \varphi_{\mathrm{s,THz}})), \end{aligned} \tag{3}$$

where η takes any losses, e.g. the photoconductor's lifetime roll-off, of the mixing product into account. The PCA output current is fed to the IF chain with a low pass cut-off frequency in the MHz-range, that can be matched to the combined linewidth of the lasers. Therefore, only the low frequency component, i.e. the difference frequency component survives as long as it is within the bandwidth (BW) of the IF chain, $BW_{\mathrm{IF}} \geq |\omega_{\mathrm{L,THz}} - \omega_{\mathrm{s,THz}}|$.

The IF chain consists of a TIA followed by digitization by an analog-digital conversion card (ACQC). Any further data processing takes place by software, including noise filtering and, most importantly, obtaining the spectral power by calculating the square of the received signal. The latter is essential as there is no phase locking between the LO and the SUT, their relative phase is random. The square, however, discards any phase information but maintains the information on spectral power within $2BW_{\mathrm{IF}}$, therefore measuring the power within a bandwidth of $2BW_{\mathrm{IF}}$. The factor of two arises from the fact that the system cannot distinguish whether the LO frequency is below or above the signal frequency.

TABLE 1. TIA and ACQC settings.

	Femto DHPCA-100				PDA-S
Measurement setting	1	2	3	4	5
TIA gain $\left(\frac{V}{A}\right)$	10^3	10^4	10^5	10^6	10^6
TIA BW (MHz)	80	14	3.5	1.8	0.15
Acquisition rate (MSa/s)	80	30	10	5	5
Digital filter BW (MHz)	40	14	3.5	1.8	1
IF BW (MHz)	40	14	3.5	1.8	0.15
RBW (MHz)	80	28	7	3.6	1.2

To measure a full spectrum of an incoming signal, the LO is swept in frequency steps of $f_{\mathrm{step}} = 2BW_{\mathrm{IF}}$ over the frequency range to be analyzed, capturing the whole spectrum without interruptions. At each frequency point, the ACQC samples n times, the samples are digitally filtered, squared and averaged in order to obtain the power. The time required for one frequency step is thus $t_{\mathrm{avg}} = n/f_{\mathrm{ACQC}}$, from now on termed as averaging time. As all spectral components falling within $2BW_{\mathrm{IF}}$ are rectified and measurement points are taken every $2BW_{\mathrm{IF}}$, the system is also capable of measuring the spectral density of true broadband sources with bandwidths far beyond $2BW_{\mathrm{IF}}$.

III. EXPERIMENTAL RESULTS

A. EXPERIMENTAL PSA IMPLEMENTATION

The experimentally realized PSA consists of two telecom (∼1550 nm) DFB lasers, controlled by a TeraScan DLC smart by TOPTICA Photonics in order to provide LO frequencies between ∼0 GHz and 1.25 THz with minimum steps of 1 MHz. The self-heterodyne linewidth of the lasers is on the order of 650 kHz, while the measured ms-time scale linewidth/frequency stability is about 1 MHz. Our PCA [11] is packaged within a fiber-pigtailed housing that utilizes a collimator and an achromatic lens to focus the laser onto the PCA. The free-space SUT is focused via a silicon lens onto it. As TIA either a Femto DHPCA-100 or a TEM Messtechnik PDA-S is used. An Advantech PCIE-1840L serves as ACQC, allowing us to add a digital low-pass filter with a stopband attenuation of at least 100 dB. Table 1 shows the used specifications of the TIA (gain and BW), ACQC (acquisition rate) and digital filter (BW) and the resolution bandwidth (RBW). Using smaller IF-BWs allows to improve the frequency resolution at cost of measurement speed.

B. PSA CHARACTERIZATION

In order to demonstrate the PSA, calibrate its spectral responsivity, determine its noise floor, and confirm its linearity, the electromagnetic wave emitted by a backward wave oscillator (BWO) (ELVA-1 G4-143e) is used as the THz-SUT. The BWO source setup consists of the following components: The BWO, a subsequent isolator (Millitech FBI-10-RSEBO), a tunable, waveguide-based attenuator (ELVA-1 VCVA-10) and a 20-dB coupler (Sage Millitech Inc. SWD 2040H-10-SB) as shown in Fig. 2. The forward output of the

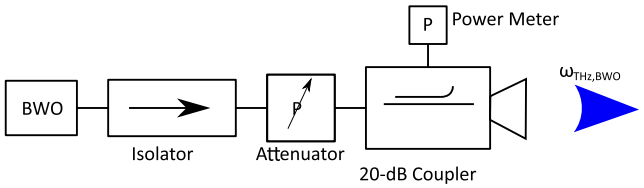

FIGURE 2. Used BWO configuration.

coupler is fed into a horn antenna towards the PSA and the −20 dB output into a Keysight N1914A power meter with a W8486A power sensor to confirm the consistency of the BWO power. To collimate and refocus the THz beam two TPX lenses are placed between the horn antenna and the PCA of the PSA. For all the measurements performed with the BWO its nominal frequency is set to 98.62 GHz and its power to 3.1 dBm, measured at the position of the PCA without attenuation.

1) CALIBRATION, RESOLUTION BANDWIDTH (RBW)

In a first step, we calibrate both the Keysight N1914A power meter reference arm as well as the responsivity of the PSA, i.e. the signal strength at a given input power. Therefore, the power of the BWO setup was recorded at the position of the PCA using a pyroelectric detector (SLT Sensor und Lasertechnik GmbH THz 10). The broadband pyroelectric detector was calibrated at the physikalisch-technische Bundesanstalt (PTB), Germany, at a frequency of 1.4 THz. We assume a maximum systematic error of 30% in the calibrated responsivity value of the detector due to the difference in the frequency emitted by the BWO and the frequency at which the calibration was performed. The noise floor of the pyroelectric detector is 8 μW. Power levels below are extrapolated using the attenuation factors given by the specifications of the waveguide attenuator. These have been confirmed independently with relative measurements. Additionally, the absolute frequency of the BWO was confirmed with our Hz-level accurate EO comb system [9].

Subsequently, we use the power recording of the pyroelectric detector to calibrate the spectral responsivity of the PSA at this frequency by matching the power of the pyroelectric detector with the integrated spectral power measured by the PSA. For simplicity, we employ a Lorentzian fit, which resembles the spectral shape of the BWO peak with an average root mean squared relative error of 12.5 % [16]. Fig. 3 shows the calibrated power spectrum of the BWO at −34.9 dBm input power, acquired with an IF BW of 150 kHz (table 1, setting 5), an averaging time of 20 ms and a f_{step} of 1 MHz. It shows a linewidth of approximately 1.2 MHz, however, this is the combined linewidth of the BWO and the LO. Since the linewidth of the BWO is expected to be in the range of some 10 kHz according to [17], the determined linewidth originates almost exclusively from the LO, which in turn is the minimum resolution bandwidth (RBW) achievable with this PSA. As the 1.2 MHz LO linewidth is about a factor of 8 wider than the IF BW for the case of $BW_{IF} = 150$ kHz (table 1, setting 5), the PSA just captures a fraction of the

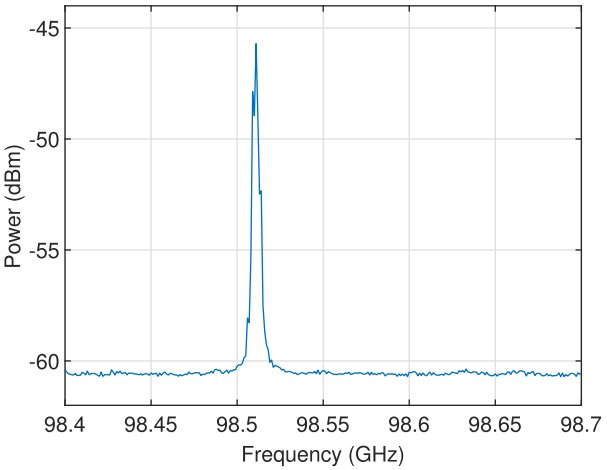

FIGURE 3. Measured BWO spectrum with 150 kHz IF BW at −34.9 dBm.

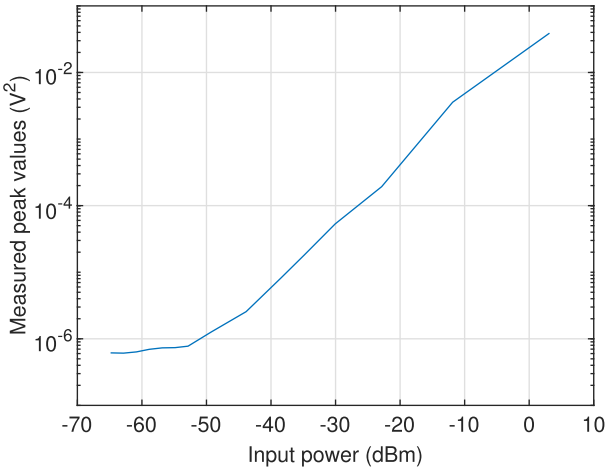

FIGURE 4. Peak measured values of the BWO spectra over the input power.

power per frequency point as it is undersampled. With a narrow band laser, we would therefore expect a 9 dB higher signal strength at $BW_{IF} = 150$ kHz.

2) LINEARITY AND 1-dB COMPRESSION POINT, DISPLAYED AVERAGE NOISE LEVEL

We record spectra of the BWO from the maximum available power of 3.1 dBm down to the detection limit. As an attenuator was used instead of tuning the BWO power, the line shape does not change. We can therefore utilize the peak amplitude of the measured spectra as a measure of power. Fig. 4 shows excellent linearity of the PSA down to −53.2 dBm of BWO power. With lower input power, the signal flattens out, finally reaching the noise power of −62.0 dBm. To calculate the DANL we have to divide the noise power for one single frequency point by the corresponding IF BW, in this case 150 kHz (table 1, setting 5), giving us a DANL of −113.8 dBm/Hz. We remark that this value is in excellent agreement with the NEP of the PCA. In [11] we have obtained a NEP of 1.8 fW/Hz (−117.4 dBm/Hz) at 188.8 GHz for a similar device using the same broadband antenna featuring a spectral waviness of

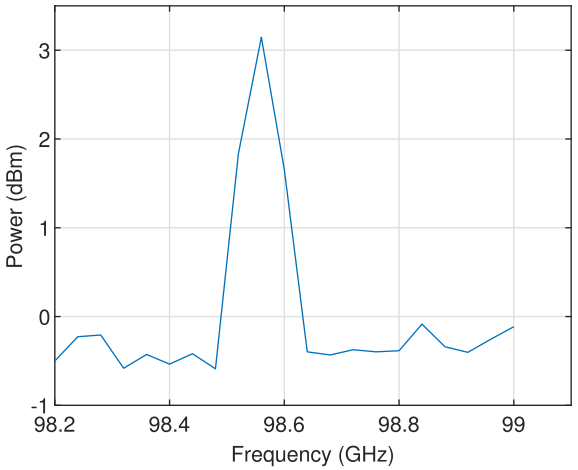

FIGURE 5. BWO spectrum measured with 40 MHz IF BW at 3.1 dBm.

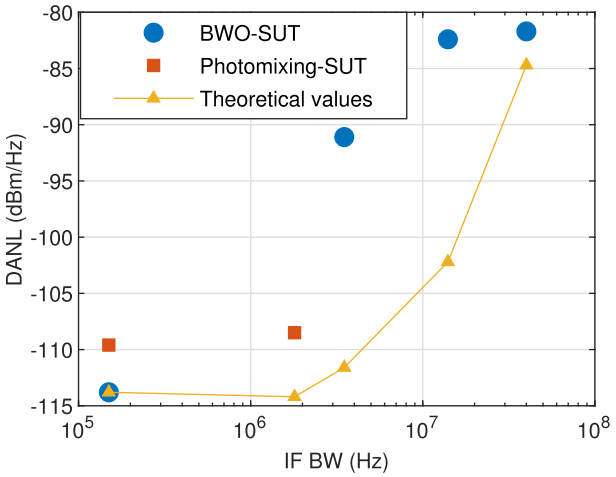

FIGURE 6. DANL for different measurement BWs at 100 GHz.

the order of 3 dB. Further the used measurement setups and therefore the noise performances of the used equipments vary. From a simplified noise study of the PSA - details will follow later - we conclude that with these settings (table 1, setting 5) the detector is the noise-limiting device and this is therefore the fundamental DANL of the system. The maximum power of the BWO at 3.1 dBm at the entrance to our PSA does not allow to determine the 1-dB compression point of the PSA which must therefore be higher than 3 dBm.

3) LARGER RBWS, MEASUREMENT SPEED

So far we only showed results with measurement setting 5 (table 1) where the RBW is limited to 1.2 MHz by the spectral purity of the lasers. The Femto TIA enables IF BWs up to 40 MHz with RBWs up to 80 MHz (table 1, setting 1). Fig. 5 shows a measurement with a BWO power of 3.1 dBm, at the maximum IF BW of 40 MHz (RBW 80 MHz) with an averaging time of 1 ms. Despite the higher input power as compared to the shown result in Fig. 3, the signal-to-noise ratio (SNR) is significantly lower and the DANL has increased to −81.7 dBm/Hz.

The main reason for the 32.1 dB decrease in DANL is the 30 dB lower TIA gain at an IF BW of 40 MHz compared to the TIA gain at an IF BW of 150 kHz. While the measurement was limited by the detector noise in case of the 150 kHz IF bandwidth, the lower TIA gain is insufficient to amplify the signal beyond the combined noise floor of the ACQC, $U_{n,ACQC}$, and the TIA. The total noise of the PSA can be calculated by

$$U_{n,PSA} = \sqrt{\left(\sqrt{\left(I_{n,Det}^2 + I_{n,TIA}^2\right)} \cdot G\right)^2 + U_{n,ACQC}^2}, \quad (4)$$

with G being the TIA transimpedance gain, $I_{n,Det} = NEI \cdot \sqrt{BW_{IF}}$ the fundamental current noise of the photoconductor with a device-specific noise equivalent current NEI, and $I_{n,TIA}$ the input current noise of the TIA. For calculation purposes, the NEI is assumed to being constant for all used BW_{IF} (table 1) and not influenced by the laser noise. At low transimpedance gain, the total system noise becomes higher than the detector noise, characterized by the excess noise (EN) added by the system of

$$EN = \frac{U_{n,PSA}}{I_{n,Det} \cdot A}. \quad (5)$$

With an estimated NEI of the detector of 4 pA/$\sqrt{\text{Hz}}$ [11], the TIA noise from the data sheet and the measured noise data from the ACQC, the EN at 150 kHz IF BW is 0.6 dB and therefore, as stated above, basically limited by the detector noise only. In contrast, the EN at 40 MHz IF BW is 29.1 dB and therefore clearly TIA- and ACQC-limited. We added theoretical values based on the EN calculations and the minimum measured DANL with the results from the BWO measurements and the results of the measurements from the photomixing SUT at 100 GHz, which is covered in the next section, to Fig. 6. While the difference in DANL between the lowest and highest IF BWs match nicely, the intermediate IF BWs of 3.5 MHz (table 1, setting 3) and 14 MHz (table 1, setting 2) show a clear discrepancy of about 20 dB. This difference is due to differences of the actual noise within the components, and neglected phase noise of the lasers but also due to interferences and clutter, that our noise model does not account for.

In summary, we reach the fundamental DANL at the IF BW of 150 kHz and are close to it for an IF BW of 1.8 MHz (table 1, setting 4). For higher IF BWs, both maximum RBW and TIA gain must be improved, e.g., by replacing the acquisition card and the TIA with more powerful commercially available options. For boosting the TIA, also a further low noise preamplifier can be employed in the IF path. The latter is a common technique for recovering the system DANL, frequently employed in electronic SAs. Further, improved shielding for incoupling of external RF noise and clutter may be required. The recovery of the DANL at IF BWs >2 MHz as well as increasing the IF BW is part of future work. Larger IF-BWs allow to increase the f_{step} without loss in information. This in turn reduces the total measurement time substantially, from e.g. about a minute for

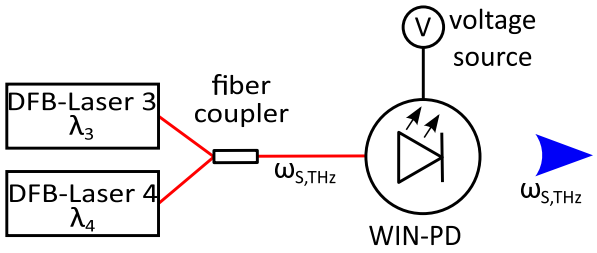

FIGURE 7. Setup of the CW source under test based on a TOPTICA photomixing setup.

a scan range of 300 MHz at a step size of 1 MHz with an IF BW of 150 kHz (Fig. 3) to less than 5 s at a step size of 40 MHz with an IF BW of 40 MHz (Fig. 5).

4) FREQUENCY COVERAGE, APPLICATIONS

In order to characterize the PSA at higher frequencies we employ a CW-THz signal generated by another photomixing setup. A commercial waveguide-integrated photodiode (WIN-PD; Fraunhofer Heinrich Hertz Institute/TOPTICA Photonics AG) is excited by the difference frequency of a set of telecom wavelength DFB lasers, controlled by a Toptica DC110 (Fig. 7). The photodiode is reverse-biased with a voltage of −1 V close to its optimum operation point. The laser system driving the SUT and the PSA are different ones and are not mutually coherent.

Similar to the BWO measurements, the CW measurements also require power measurements to calibrate the data. These are done using a Golay cell (Tydex GC1) with a noise floor of 1 nW for a frequency range from 100 GHz to 1050 GHz. For calibration, the Golay cell was referenced to power measurements with the PTB-calibrated pyroelectric detector (same as in the BWO case) at two frequencies. The power of the WIN-PD varies between 1 μW at 1 THz and 60 μW at 150 GHz, which is significantly lower than the maximum power achievable with the BWO.

After the power measurements, the PSA records the spectrum of the SUT using an IF BW of 150 kHz (table 1, setting 5) with an averaging time of 10 ms. The frequency sweep is set up as follows: First, the transmitter frequency is set to a defined value, starting at 96 GHz and going up in steps of 50 GHz until the maximum measurable frequency of 1046 GHz is reached. At each step, the PSA records a spectrum around the expected frequency with frequency steps of 1 MHz within a frequency interval of at least 300 MHz. As the power of the emitter substantially rolls off towards higher frequencies, being close to the PSA noise floor at the upper end of the spectra, the presence of the signal was verified by repeating the measurement several times. Figs. 8 and 9 depict exemplary spectra. The recorded spectra reveal a miscalibration of the emitter frequency.

Fig. 8 shows the SUT at a set frequency of 1046 GHz, which appears at a frequency of 1050 GHz. The offset is due to a miscalibration of the look-up table mainly of the SUT and can easily be fixed by recalibrating both the SUT and the LO look-up table, e.g. with the aid of water vapor

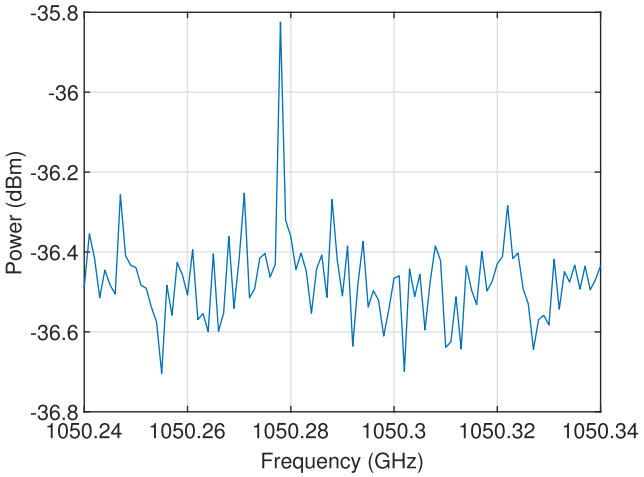

FIGURE 8. Spectrum of the CW P-I-N diode photomixer around 1050.3 GHz.

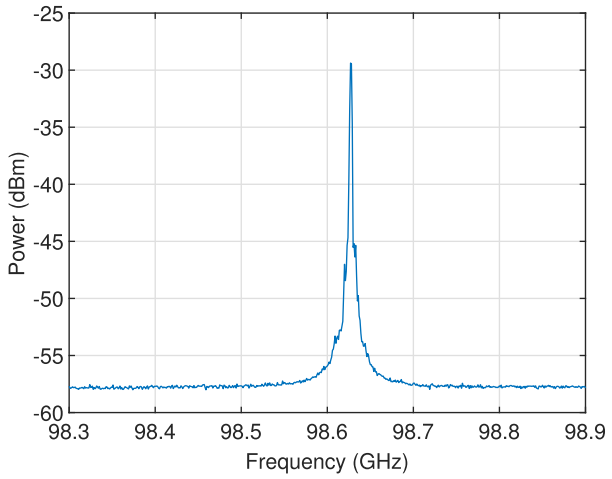

FIGURE 9. Spectrum of the CW P-I-N diode photomixer around 98.6 GHz.

resonances or by live-monitoring the wavelengths with a wavemeter or optical spectrum analyzer. For the PSA LO, the water vapor resonances between 557 GHz and 1,114 GHz as well as an electro-optic comb system at 98.6 GHz are used for calibration. The water lines measured with the PSA LO agreed excellently with the HITRAN data base. At the lower end of the spectrum, however, the measurement with the EO comb showed a discrepancy of 1.4 GHz.

Both exemplary spectra (Fig. 8,9) are well approximated with a Lorentzian shape with a combined linewidth of approximately 1.5 MHz, which is used to calculate the power values. Assuming both the LO of the SUT and of the SA have a linewidth of 1.2 MHz, like earlier determined, the measured combined linewidth comes close to the expected value of $\sqrt{2}\cdot 1.2\,\text{MHz} = 1.7\,\text{MHz}$ [18]. Fig. 10 depicts the responsivity from the peak spectral values and the corresponding input power levels. With increasing frequency the responsivity of the SA decreases. This is mainly due to the roll-offs within the PCA [15]. Said effects and any potential voltage offsets at the ACQC will be the limiting factors for the maximum detectable frequency. Due to the squaring of the measured

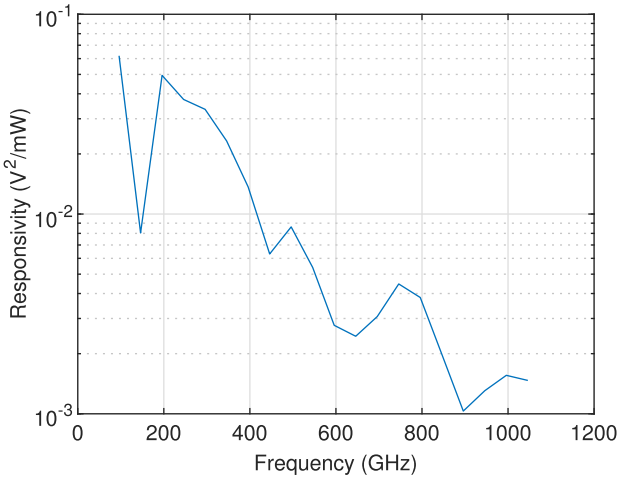

FIGURE 10. Spectral responsivity of the PSA.

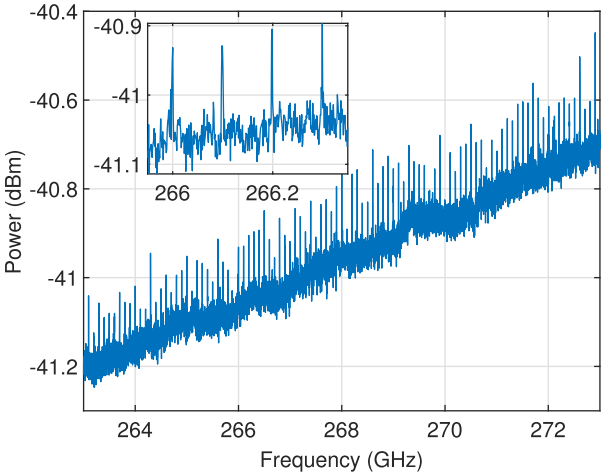

FIGURE 11. Spectrum of the pulsed SUT from 263 GHz to 273 GHz with zoomed-in spectrum showing the individual modes.

voltages to get power relatable data, any measured offset will also determine the noise floor of the PSA. We remark that the maximum measurable frequency of 1050 GHz is due to a combination of PSA noise floor and limited SUT power. The maximum tuning range of the current PSA system is 1250 GHz, defined by the tuning range of the DFB laser diodes of the LO. For SUTs with higher power at and above 1050 GHz, compared with the SUT shown here, a replacement of one of the DFB diodes with an external cavity laser or a VCSEL [19] would allow for a frequency coverage up to several THz. According to the roll-offs of the PCA, the DANL is expected to increase as f^4 towards higher frequencies beyond 1 THz, possibly more when leaving the design range of the logarithmic-periodic antenna. A redesign and optimization of the PCA antenna structure, however, would allow for optimization of the system at a specific target frequency.

C. APPLICATION EXAMPLE: PULSED THz SIGNAL

So far we only investigated CW-SUTs that can be resolved with a small measurement BW. With a pulsed THz signal we demonstrate that also signals covering a large bandwidth can be resolved. The pulsed THz signal is generated by an ErAs:InAlGaAs PCA [20] that is driven by a fiber-coupled mode-locked laser (Menlo C-fiber System) with an optical power of 42 mW and a repetition rate of approximately 100 MHz. The photomixer is biased with a voltage of 200 V. Fig. 11 shows the measured spectrum for frequencies from 263 to 273 GHz with a step size of 1 MHz at an IF BW of 150 kHz (table 1, setting 5) and an averaging time of 10 ms. This leads to a total measurement time of four hours, which is mainly caused by taking 100,001 frequency points. The resulting values are mapped to power values using the receiver's responsivity, which creates the slope within the noise floor. From the inset of Fig. 11 the comb-like structure of the pulsed system is visible with a spacing of the peaks that corresponds to the repetiton rate of slightly less than 100 MHz.

IV. COMPARISON TO ELECTRONIC SPECTRUM ANALYZERS

A clear downside of the PSA as compared to a frequency-extended ESA is the minimum RBW of 1.2 MHz whereas ESAs offer RBWs below 1 kHz. Still, for many applications, the minimum RBW is sufficient. Hz-level RBWs are possible by employing CW frequency combs as demonstrated in [9] and [10], which result in extremely accurate but also very timely measurements. The maximum RBW demonstrated in this paper is only limited by the speed of the acquisition card and the gain-bandwidth product of the TIA. Employing faster components or FPGAs in conjunction with LNAs will allow to trim the RBW to several GHz, comparable to ESAs, and may even allow to recover the system DANL at these high measurement speeds. Similar to an ESA, the photonic SA is able to characterize any arbitrary signal and is able to operate at room temperature without any special cooling. The data are obtained in the frequency domain. The lowest resolved input power at 100 GHz of −58.9 dBm at a RBW of 1.2 MHz is still three to four orders of magnitude worse than an equivalent ESA. This discrepancy becomes smaller at higher THz frequencies. In terms of frequency coverage, an electronic SA requires at least 6 extenders to cover the frequency range from microwaves up to 1 THz. The presented photonic SA covers 1.25 THz bandwidth using only thermally stabilized DFB diodes. A frequency coverage of several THz with a single system is easily feasible, e.g. by employing external cavity lasers. As the presented system is operated with 1550 nm technology, it profits fully from highly developed and comparatively affordable telecom components and lasers. The photonic SA is therefore less expensive than the base ESA unit without any extenders.

V. CONCLUSION

We have demonstrated a photonic SA, for free-space signal-under-tests, composed of an optical LO and a photoconductive mixer. The system is thoroughly characterized with respect to the key characteristics: It features an extremely wide frequency coverage of 1.25 THz that can easily be

extended to several THz with minor modifications. The RBW is freely selectable within 1.2 MHz and 80 MHz, yet limited by the post detection hardware. The achieved displayed average noise level at 100 GHz is −113.8 dBm, close to the theoretically achievable noise floor with the employed photoconductor. The DANL increases with increasing frequency depending on the performance of the photoconductive mixer. The 1-dB compression point is higher than 3 dBm and could not be determined with the power levels of the investigated SUTs. The PSA architecture is fully compatible with state-of-the-art photomixing systems, only requiring modifications in the IF readout chain. For demonstrating the PSA performance, we have characterized three different mm-wave and THz sources: a backward wave oscillator operating in the W-band, a continuous-wave photomixer between 50 GHz and 1050 GHz, and a pulsed photoconductor between 200 and 300 GHz.

REFERENCES

[1] M. Z. Chowdhury, M. Shahjalal, S. Ahmed, and Y. M. Jang, "6G wireless communication systems: Applications, requirements, technologies, challenges, and research directions," *IEEE Open J. Commun. Soc.*, vol. 1, pp. 957–975, 2020.
[2] H. Iida, M. Kinoshita, and Y. Tojima, "Terahertz spectrum analyzer based on Fourier transform interferometry," *J. Infr., Millim., THz Waves*, vol. 40, no. 9, pp. 952–961, Sep. 2019.
[3] Y. Jiang, M. Liang, B. Jin, L. Kang, W. Xu, J. Chen, and P. Wu, "A simple Fourier transform spectrometer for terahertz applications," *Chin. Sci. Bull.*, vol. 57, no. 6, pp. 573–578, Feb. 2012.
[4] Y. Divin, M. Lyatti, and U. Poppe, "Hilbert spectral analysis of THz radiation sources by high-Tc Josephson detectors," *Phys. Proc.*, vol. 36, pp. 166–171, Jan. 2012.
[5] R. Schwarz. *FSW Signal and Spectrum Analyzer*. Rhode & Schwarz Website. Accessed: Apr. 12, 2022. [Online]. Available: https://www.rohde-schwarz.com/U.K./products/test-and-measurement/benchtop-analyzers/rs-fsw-signal-and-spectrum-analyzer_63493-11793.html?change_c=true
[6] V. Diodes. *Spectrum Analyzer Extension Modules*. Virginia Diodes, Inc. Website. Accessed: Apr. 12, 2022. [Online]. Available: https://www.vadiodes.com/en/products/spectrum-analyzer
[7] T. Yasui, R. Nakamura, K. Kawamoto, A. Ihara, Y. Fujimoto, S. Yokoyama, H. Inaba, K. Minoshima, T. Nagatsuma, and T. Araki, "Real-time monitoring of continuous-wave terahertz radiation using a fiber-based, terahertz-comb-referenced spectrum analyzer," *Opt. Exp.*, vol. 17, no. 9, pp. 17034–17043, 2009.
[8] S. Yokoyama, R. Nakamura, M. Nose, T. Araki, and T. Yasui, "Terahertz spectrum analyzer based on a terahertz frequency comb," *Opt. Exp.*, vol. 16, no. 17, pp. 13052–13061, 2008.
[9] A. D. J. F. Olvera, B. L. Krause, and S. Preu, "A true optoelectronic spectrum analyzer for millimeter waves with Hz resolution," *IEEE Access*, vol. 9, pp. 114339–114347, 2021.
[10] A. D. J. F. Olvera, B. L. Krause, A. Betancur-Perez, U. Nandi, C. de Dios, P. Acedo, and S. Preu, "Frequency selective optoelectronic downconversion of a terahertz pulse using ErAs: In(Al)GaAs photoconductors," *IEEE Access*, vol. 9, pp. 95391–95400, 2021.
[11] A. D. J. F. Olvera, A. Roggenbuck, K. Dutzi, N. Vieweg, H. Lu, A. C. Gossard, and S. Preu, "International system of units (SI) traceable noise-equivalent power and responsivity characterization of continuous wave ErAs:InGaAs photoconductive terahertz detectors," *Photonics*, vol. 6, no. 1, pp. 15–27, 2019.
[12] E. Prior, C. de Dios, R. Criado, M. Ortsiefer, P. Meissner, and P. Acedo, "1THz span optical frequency comb using VCSELs and off the shelf expansion techniques," in *Proc. Conf. Lasers Electro-Optics*, Jun. 2016, pp. 1–2.
[13] S. Preu, "Device and method for spectral analysis," U.S. Patent 10 866 141, Dec. 15, 2020.
[14] S. Preu, G. H. Döhler, S. Malzer, L. J. Wang, and A. C. Gossard, "Tunable, continuous-wave terahertz photomixer sources and applications," *J. Appl. Phys.*, vol. 109, no. 6, Mar. 2011, Art. no. 061301.
[15] G. Carpnitero, L. E. G. Muñoz, H. L. Hartnagel, S. Preu, and A. V. Räisänen, *Semiconductor Terahertz Technology, Devices and Systems at Room Temperature Operation*, 1st ed. Chichester, U.K.: Wiley, 2015.
[16] M. Despotovic, V. Nedic, D. Despotovic, and S. Cvetanovic, "Evaluation of empirical models for predicting monthly mean horizontal diffuse solar radiation," *Renew. Sustain. Energy Rev.*, vol. 56, pp. 246–260, Apr. 2016.
[17] F. Lewen, R. Gendriesch, I. Pak, D. G. Paveliev, M. Hepp, R. Schieder, and G. Winnewisser, "Phase locked backward wave oscillator pulsed beam spectrometer in the submillimeter wave range," *Rev. Sci. Instrum.*, vol. 69, no. 1, pp. 32–39, Jan. 1998.
[18] G. Cicogna, *Exercises and Problems in Mathematical Methods of Physics*, 2nd ed. Cham, Switzerland: Springer, 2020.
[19] M. T. Haidar, S. Preu, S. Paul, C. Gierl, J. Cesar, A. Emsia, and F. Küppers, "Widely tunable telecom MEMS-VCSEL for terahertz photomixing," *Opt. Lett.*, vol. 40, no. 19, p. 4428, 2015.
[20] U. Nandi, F. R. Faridi, A. D. J. F. Olvera, J. Norman, H. Lu, A. C. Gossard, and S. Preu, "High dynamic range THz systems using ErAs:In(Al)GaAs photoconductors," in *IEEE MTT-S Int. Microw. Symp. Dig.*, Jul. 2019, pp. 115–117.

BENEDIKT LEANDER KRAUSE received the B.Sc. degree in electronic and sensor materials from Technical University Bergakademie Freiberg (TUBAF), Freiberg, Germany, in 2015, and the M.Sc. degree in electrical engineering from Friedrich-Alexander University Erlangen-Nürnberg (FAU), Erlangen, Germany, in 2019. He is currently pursuing the Ph.D. degree with the Terahertz Devices and Systems Laboratory, Technical University Darmstadt, Darmstadt, Germany. His research interest includes the development of photonic-based spectrum analyzers using photoconductive mixers for the terahertz range.

ANUAR DE JESUS FERNANDEZ OLVERA received the B.Sc. degree in electronic and computer engineering from the Monterrey Institute of Technology and Higher Education (ITESM), Mexico, in 2010, and the M.Sc. degree in electrical engineering from the Eindhoven University of Technology (TU/e), Eindhoven, The Netherlands, in 2015. He is currently pursuing the Ph.D. degree with the Terahertz Devices and Systems Laboratory, Technical University Darmstadt, Darmstadt, Germany. His research interests include the development of terahertz systems and applications using photoconductive mixers and their theoretical modeling.

SASCHA PREU (Member, IEEE) received the Diploma and Ph.D. degrees *(summa cum laude)* in physics from the University of Erlangen-Nuremberg, Erlangen, Germany, in 2005 and 2009, respectively. From 2004 to 2010, he was with the Max Planck Institute for the Science of Light, Erlangen. From 2010 to 2011, he worked with the Materials and Physics Department, University of California at Santa Barbara, Santa Barbara, CA, USA, in the framework of a Feodor Lynen stipend by the Humboldt foundation. From 2011 to 2014, he was with the Chair of Applied Physics, University of Erlangen-Nuremberg. He is currently a Full Professor with the Department of Electrical Engineering and Information Technology, Technical University Darmstadt, Darmstadt, Germany, where he is leading the Terahertz Devices and Systems Laboratory. His current research interests include the development of semiconductor-based terahertz sources and detectors, including photomixers, photoconductors, and field-effect transistor rectifiers, spintronic devices, development of powerful terahertz systems, and applications of terahertz radiation. In 2017, he received an ERC starting grant for developing ultra-broadband and photonic terahertz signal analyzers.